ELSEVIER

International Journal of Solids and Structures 41 (2004) 4697–4712

INTERNATIONAL JOURNAL OF SOLIDS and STRUCTURES

www.elsevier.com/locate/ijsolstr

3-D vibration analysis of generalized super elliptical plates using Chebyshev–Ritz method

D. Zhou [a], S.H. Lo [b], Y.K. Cheung [b,*], F.T.K. Au [b]

[a] *Department of Mechanics and Engineering Science, Nanjing University of Science and Technology, Nanjing 210014, People's Republic of China*

[b] *Department of Civil Engineering, The University of Hong Kong, Pokfulam Road, Hong Kong, People's Republic of China*

Received 16 July 2003; received in revised form 19 January 2004

Available online 12 April 2004

Abstract

The three-dimensional free vibration of generalized super elliptical plates is analysed, based on the exact, small-strain and linear elasticity theory. The Ritz method is applied to derive the frequency equation. The triplicate Chebyshev polynomial series form the backbones of the admissible functions, as modified by a characteristic boundary function to ensure the satisfaction of geometric boundary conditions of the plate. Utilizing the symmetry of the plate under consideration, eight distinct vibration modes can be classified and individually solved while maintaining the same level of accuracy. The accuracy of the present method has been examined by the convergence and comparison studies. The effect of geometric parameters on vibration behaviour of the generalized super elliptical plates with free and fixed perimeters have been studied for different powers, thickness ratios and aspect ratios.

1. Introduction

The analysis of vibration characteristics of plates with various shapes has attracted the interests from a lot of researchers because of their applications in various branches of engineering. In the Cartesian coordinate system, the perimeter F of a generalized super elliptical plate, as shown in Fig. 1, is defined by

$$F(x,y) = \left(\frac{2x}{a}\right)^{2n_x} + \left(\frac{2y}{b}\right)^{2n_y} - 1 = 0, \quad n_x, n_y = 1, 2, 3, \ldots \tag{1}$$

where a and b are the maximum dimensions of the plate in the x and y directions, respectively. The above equation can describe a type of common plates by giving different values to the integer powers n_x and n_y, and the aspect ratio a/b. For example, setting $n_x = n_y = 1$ and $a/b = 1$ gives a circular plate, while prescribing $n_x = n_y = 1$ and $a/b \neq 1$ represents an elliptical plate. It is obvious that the higher values of n_x

* Corresponding author. Tel.: +852-2859-2668; fax: +852-2559-5337.
E-mail address: hreccyk@hkucc.hku.hk (Y.K. Cheung).

0020-7683/$ - see front matter © 2004 Published by Elsevier Ltd.
doi:10.1016/j.ijsolstr.2004.02.045

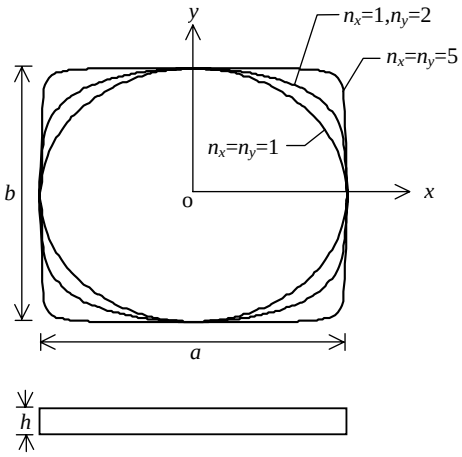

Fig. 1. Geometry and dimensions of a generalized super elliptical plate.

and/or n_y correspond to a smaller corner radius. Therefore, the perimeter of the plate approaches a rectangular one with increase in the powers. In a sense, the present work on super elliptical plates provides a unified treatment for a wide range of plates ranging from circular plates, elliptical plates to rectangular plates by setting suitable indices.

Some investigations have been carried out on vibration of super elliptical plates due to their importance in engineering applications. Sato (1971) used the analytical method and Narita (1985) used the Ritz method to study isotropic and orthotropic elliptical plates based on the classical thin plate theory, respectively. Wang et al. (1994) studied the vibration and buckling of super elliptical thin plates, while DeCapua and Sun (1972) studied the eigenfrequencies of orthotropic super elliptical thin plates using the 2-D simple algebraic polynomials as the admissible functions in the Ritz method. Irie et al. (1983) combined the conformal mapping technique with Ritz method to study the vibration of square membrane and thin plate with rounded corners. Rajalingham et al. (1993) studied the free vibration of elliptical thin plates by using the orthogonal polynomials and trigonometric functions as the admissible functions in a modified polar coordinate system. Liew et al. (1998b) and Chen et al. (1999) studied the free vibration of isotropic and symmetric laminated thick super elliptical plates by using the higher-order shear deformation plate theory in the Ritz method, respectively. Moreover, the free vibration of isotropic and laminated, thin and thick perforated plates have been studied by Lim and Liew (1995), Lim et al. (1998) and Chen et al. (2000) using the classical thin plate theory and the higher-order shear deformation plate theory, respectively.

In the recent two decades, the 3-D vibration analysis of plates based on the exact, small strain and linear elasticity theory has received increasing attention as such methods are applicable not only to thin plates, but also to moderately thick and thick plates. Among various numerical methods, the Ritz method shows some advantages in both the accuracy and the convenience. Simple algebraic polynomials (Leissa and Zhang, 1983; So and Leissa, 1998), generated orthogonal polynomials (Liew et al., 1993; Liew and Yang, 2000) and Chebyshev polynomials (Zhou et al., 2002; Zhou et al., 2003) were taken as the admissible functions and have been demonstrated effective. Liew et al. (1995a) studied the 3-D vibration of elliptical bars and recently, Liew and Feng (2001) studied the 3-D vibration of perforated super elliptical plates using the 1-D and 2-D generated orthogonal polynomials as the admissible functions. Moreover, the 3-D vibration of plates with various shapes have been analysed by the Ritz method (Leissa and Jacob, 1986; Cheung and Zhou, 2002; Zhou et al., 2003; Young and Dickinson, 1994, 1995; Liew et al., 1994, 1998a, 1995b).

It is obvious that Eq. (1) describes a more far-reaching type of plates than super elliptical plates. For the case of $n_x = n_y$, the generalized super elliptical plates degenerate into super elliptical plates which have been

studied by some researchers (Liew et al., 1998b; Chen et al., 1999; Wang et al., 1994; DeCapua and Sun, 1972; Irie et al., 1983). In the present study, the 3-D free vibrations of generalized super elliptical plates are considered. The triplicate Chebyshev polynomials multiplied by a characteristic boundary function for each displacement component are taken as the admissible functions. Convergence and comparison studies demonstrate the accuracy and the correctness of the present method. The effect of the geometric parameters such as the thickness ratio, aspect ratio and powers on the frequency parameters has been investigated in detail.

2. Formulation

Consider a generalized super elliptical plate as shown in Fig. 1 with a Cartesian coordinate system $x-y-z$. The plate is made of isotropic material and has a uniform thickness h. The shape of the plate is controlled by two positive integers n_x and n_y, and the aspect ratio a/b. It is obvious that no matter what values n_x and n_y are assigned, the plate always stays within a rectangular hexahedral domain with the sides a, b and h. For the case of $a=b$, the hexahedral domain has a square planform.

Based on the exact, small strain, and 3-D linear elasticity theory, the elastic strain energy Λ and the kinetic energy T of the plate can be written in the volume integral form as

$$\Lambda = \frac{E}{2(1+\nu)} \int_{-a/2}^{a/2} \int_{-r}^{r} \int_{-h/2}^{h/2} \left(\frac{\nu}{1-2\nu} \Lambda_1 + \Lambda_2 + \frac{1}{2} \Lambda_3 \right) \mathrm{d}z\,\mathrm{d}y\,\mathrm{d}x \tag{2}$$

$$T = \frac{\rho}{2} \int_{-a/2}^{a/2} \int_{-r}^{r} \int_{-h/2}^{h/2} \left[\left(\frac{\partial u}{\partial t} \right)^2 + \left(\frac{\partial v}{\partial t} \right)^2 + \left(\frac{\partial w}{\partial t} \right)^2 \right] \mathrm{d}z\,\mathrm{d}y\,\mathrm{d}x \tag{3}$$

where $r = (b/2)\sqrt[n_y]{1-(2x/a)^{n_x}}$ and

$$\Lambda_1 = (\varepsilon_{xx} + \varepsilon_{yy} + \varepsilon_{zz})^2; \quad \Lambda_2 = \varepsilon_{xx}^2 + \varepsilon_{yy}^2 + \varepsilon_{zz}^2; \quad \Lambda_3 = \varepsilon_{xy}^2 + \varepsilon_{xz}^2 + \varepsilon_{yz}^2 \tag{4}$$

E is the Young's modulus, ν is the Poisson's ratio and ρ is the mass density per unit volume. The strain components $\varepsilon_{ij}(i,j=x,y,z)$ in the Cartesian coordinates for small deformation are given as

$$\begin{aligned} &\varepsilon_{xx} = \frac{\partial u}{\partial x}; \quad \varepsilon_{yy} = \frac{\partial v}{\partial y}; \quad \varepsilon_{zz} = \frac{\partial w}{\partial z} \\ &\varepsilon_{xy} = \frac{\partial u}{\partial y} + \frac{\partial v}{\partial x}; \quad \varepsilon_{xz} = \frac{\partial u}{\partial z} + \frac{\partial w}{\partial x}; \quad \varepsilon_{yz} = \frac{\partial v}{\partial z} + \frac{\partial w}{\partial y} \end{aligned} \tag{5}$$

In the free vibration of the plate, its periodic displacement components can be expressed in terms of the time t as

$$\begin{aligned} &u(x,y,z,t) = U(x,y,z)\mathrm{e}^{\mathrm{i}\omega t}; \quad v(x,y,z,t) = V(x,y,z)\mathrm{e}^{\mathrm{i}\omega t} \\ &w(x,y,z,t) = W(x,y,z)\mathrm{e}^{\mathrm{i}\omega t} \end{aligned} \tag{6}$$

where $U(x,y,z)$, $V(x,y,z)$ and $W(x,y,z)$ are the displacement amplitude functions, ω denotes the natural frequency of the plate and $i=\sqrt{-1}$.

For simplicity and convenience in mathematical formulation, the following non-dimensional parameters are introduced

$$\xi = 2x/a; \quad \eta = 2y/b; \quad \zeta = 2z/h \tag{7}$$

The maximum energy functional Π of the plate is defined as

$$\Pi = \Lambda_{\max} - T_{\max} \tag{8}$$

where

$$\begin{aligned} V_{\max} &= \frac{Eh}{4\lambda(1+\nu)} \int_{-1}^{1} \int_{-\bar{r}}^{\bar{r}} \int_{-1}^{1} \left(\frac{\nu}{1-2\nu} \overline{\Lambda}_1 + \overline{\Lambda}_2 + \frac{1}{2} \overline{\Lambda}_3 \right) \mathrm{d}\zeta \, \mathrm{d}\eta \, \mathrm{d}\xi \\ T_{\max} &= \frac{\rho}{16} abh\omega^2 \int_{-1}^{1} \int_{-\bar{r}}^{\bar{r}} \int_{-1}^{1} (U^2 + V^2 + W^2) \, \mathrm{d}\zeta \, \mathrm{d}\eta \, \mathrm{d}\xi \end{aligned} \tag{9}$$

in which

$$\begin{aligned} &\bar{r} = \sqrt[n_y]{1-\xi^{n_x}}, \\ &\overline{\Lambda}_1 = (\bar{\varepsilon}_{\xi\xi} + \bar{\varepsilon}_{\eta\eta} + \bar{\varepsilon}_{\zeta\zeta})^2; \quad \overline{\Lambda}_2 = \bar{\varepsilon}_{\xi\xi}^2 + \bar{\varepsilon}_{\eta\eta}^2 + \bar{\varepsilon}_{\zeta\zeta}^2; \quad \overline{\Lambda}_3 = \bar{\varepsilon}_{\xi\eta}^2 + \bar{\varepsilon}_{\xi\zeta}^2 + \bar{\varepsilon}_{\eta\zeta}^2, \\ &\bar{\varepsilon}_{\xi\xi} = \frac{\partial U}{\partial \xi}; \quad \bar{\varepsilon}_{\eta\eta} = \lambda \frac{\partial V}{\partial \eta}; \quad \bar{\varepsilon}_{\zeta\zeta} = \frac{\lambda}{\gamma} \frac{\partial W}{\partial \zeta}, \\ &\bar{\varepsilon}_{\xi\eta} = \lambda \frac{\partial U}{\partial \eta} + \frac{\partial V}{\partial \xi}; \quad \bar{\varepsilon}_{\xi\zeta} = \frac{\lambda}{\gamma} \frac{\partial U}{\partial \zeta} + \frac{\partial W}{\partial \xi}; \quad \bar{\varepsilon}_{\eta\zeta} = \frac{\lambda}{\gamma} \frac{\partial V}{\partial \zeta} + \lambda \frac{\partial W}{\partial \eta}, \\ &\lambda = a/b; \quad \gamma = h/b \end{aligned} \tag{10}$$

In the present analysis, each of the displacement amplitude functions $U(\xi,\eta,\zeta)$, $V(\xi,\eta,\zeta)$ and $W(\xi,\eta,\zeta)$ is taken, respectively, in the form of triplicate series of Chebyshev polynomials multiplied by a characteristic boundary function which ensures that the displacement component satisfies the essential geometric boundary conditions of the plate, i.e.

$$\begin{aligned} U(\xi,\eta,\zeta) &= F_u(\xi,\eta) \sum_{i=1}^{\infty} \sum_{j=1}^{\infty} \sum_{k=1}^{\infty} A_{ijk} P_i(\xi) P_j(\eta) P_k(\zeta) \\ V(\xi,\eta,\zeta) &= F_v(\xi,\eta) \sum_{l=1}^{\infty} \sum_{m=1}^{\infty} \sum_{n=1}^{\infty} B_{lmn} P_l(\xi) P_m(\eta) P_n(\zeta) \\ W(\xi,\eta,\zeta) &= F_w(\xi,\eta) \sum_{p=1}^{\infty} \sum_{q=1}^{\infty} \sum_{r=1}^{\infty} C_{pqr} P_p(\xi) P_q(\eta) P_r(\zeta) \end{aligned} \tag{11}$$

where A_{ijk}, B_{lmn} and C_{pqr} are the unknown coefficients. The 1-D sth Chebyshev polynomial $P_s(\chi)$ $(s = 1,2,3,\ldots;\chi = \xi,\eta,\zeta)$ can be written in terms of cosine functions as follows:

$$P_s(\chi) = \cos[(s-1)\arccos(\chi)]; \quad (s = 1,2,3,\ldots) \tag{12}$$

Note that $F_u(\xi,\eta)$, $F_v(\xi,\eta)$ and $F_w(\xi,\eta)$ are the characteristic boundary functions, respectively, corresponding to the displacements u, v and w.

It is obvious that the three duplicate Chebyshev polynomial series $P_i(\xi)P_j(\eta)P_k(\zeta)$ $(i,j,k,=1,2,3,\ldots)$ constitute a complete and orthogonal set in the cubic domain with two corner-point coordinates $(1,1,1)$ and $(-1,-1,-1)$. Substituting Eq. (11) into Eq. (9) and minimizing the functional Π with respect to the coefficients of the admissible functions, i.e.

$$\frac{\partial \Pi}{\partial A_{ijk}} = 0, \quad \frac{\partial \Pi}{\partial B_{lmn}} = 0, \quad \frac{\partial \Pi}{\partial C_{pqr}} = 0 \quad (i,j,k,l,m,n,p,q,r = 1,2,3,\ldots) \tag{13}$$

leads to the following governing eigenvalue equation in matrix form:

$$\left(\begin{bmatrix} [K_{uu}] & [K_{uv}] & [K_{uw}] \\ [K_{uv}]^{\mathrm{T}} & [K_{vv}] & [K_{vw}] \\ [K_{uw}]^{\mathrm{T}} & [K_{vw}]^{\mathrm{T}} & [K_{ww}] \end{bmatrix} - \Omega^2 \begin{bmatrix} [M_{uu}] & 0 & 0 \\ 0 & [M_{vv}] & 0 \\ 0 & 0 & [M_{ww}] \end{bmatrix} \right) \begin{Bmatrix} \{A\} \\ \{B\} \\ \{C\} \end{Bmatrix} = \begin{Bmatrix} \{0\} \\ \{0\} \\ \{0\} \end{Bmatrix} \tag{14}$$

in which $\Omega = \omega a\sqrt{\rho/E}$, $[K_{ij}]$ and $[M_{ii}](i,j = u,v,w)$ are the stiffness sub-matrices and the diagonal mass sub-matrices, respectively. The column vectors $\{A\}$, $\{B\}$ and $\{C\}$ contain unknown coefficients expressed in the following forms

$$\{A\} = \begin{Bmatrix} A_{111} \\ A_{112} \\ \vdots \\ A_{11K} \\ A_{121} \\ \vdots \\ A_{12K} \\ \vdots \\ A_{1JK} \\ \vdots \\ A_{IJK} \end{Bmatrix}, \quad \{B\} = \begin{Bmatrix} B_{111} \\ B_{112} \\ \vdots \\ B_{11N} \\ B_{121} \\ \vdots \\ B_{12N} \\ \vdots \\ B_{1MN} \\ \vdots \\ A_{LMN} \end{Bmatrix}, \quad \{C\} = \begin{Bmatrix} C_{111} \\ C_{112} \\ \vdots \\ C_{11R} \\ C_{121} \\ \vdots \\ C_{12R} \\ \vdots \\ C_{1QR} \\ \vdots \\ C_{PQR} \end{Bmatrix} \tag{15}$$

where I, J, K, L, M, N, P, Q and R are the truncation orders. The elements of the stiffness sub-matrices $[K_{ij}]$ and mass sub-matrices $[M_{ii}]$ $(i,j = u,v,w)$ are given by

$$\begin{aligned}
[K_{uu}] &= \frac{1-v}{1-2v} D^{1,1,0,0}_{uiju\bar{i}\bar{j}} H^{0,0}_{uku\bar{k}} + \frac{\lambda^2}{2}\left(D^{0,0,1,1}_{uiju\bar{i}\bar{j}} H^{0,0}_{uku\bar{k}} + \frac{1}{\gamma^2} D^{0,0,0,0}_{uiju\bar{i}\bar{j}} H^{1,1}_{uku\bar{k}} \right), \\
[K_{uv}] &= \lambda\left(\frac{v}{1-2v} D^{1,0,0,1}_{uijvl\bar{m}} H^{0,0}_{uku\bar{n}} + \frac{1}{2} D^{0,1,1,0}_{uijvl\bar{m}} H^{0,0}_{uku\bar{n}} \right), \\
[K_{uw}] &= \frac{\lambda}{\gamma}\left(\frac{v}{1-2v} D^{1,0,0,0}_{uijwpq} H^{0,1}_{ukwr} + \frac{1}{2} D^{0,1,0,0}_{uijwpq} H^{1,0}_{ukwr} \right), \\
[K_{vv}] &= \lambda^2\left(\frac{1-v}{1-2v} D^{0,0,1,1}_{vlmv\bar{l}\bar{m}} H^{0,0}_{vnv\bar{n}} + \frac{1}{2\gamma^2} D^{0,0,0,0}_{vlmv\bar{l}\bar{m}} H^{1,1}_{vnv\bar{n}} \right) + \frac{1}{2} D^{1,1,0,0}_{vlmv\bar{l}\bar{m}} H^{0,0}_{vnv\bar{n}}, \\
[K_{vw}] &= \frac{\lambda^2}{\gamma}\left(\frac{v}{1-2v} D^{0,0,1,0}_{vlmwpq} H^{0,1}_{vnwr} + \frac{1}{2} D^{0,0,0,1}_{vlmwpq} H^{1,0}_{vnwr} \right), \\
[K_{ww}] &= \lambda^2\left(\frac{1-v}{\gamma^2(1-2v)} D^{0,0,0,0}_{wpqw\bar{p}\bar{q}} H^{1,1}_{wrw\bar{r}} + \frac{1}{2} D^{0,0,1,1}_{wpqw\bar{p}\bar{q}} H^{0,0}_{wrw\bar{r}} \right) + \frac{1}{2} D^{1,1,0,0}_{wpqw\bar{p}\bar{q}} H^{0,0}_{wrw\bar{r}}, \\
[M_{uu}] &= (1+v) D^{0,0,0,0}_{uiju\bar{i}\bar{j}} H^{0,0}_{uku\bar{k}}/4, \\
[M_{vv}] &= (1+v) D^{0,0}_{vlmv\bar{l}\bar{m}} H^{0,0}_{vnv\bar{n}}/4, \\
[M_{ww}] &= (1+v) D^{0,0,0,0}_{wpqw\bar{p}\bar{q}} H^{0,0}_{wrw\bar{r}}/4, \quad i,j,k,l,m,n,p,q,r,\bar{i},\bar{j},\bar{k},\bar{l},\bar{m},\bar{n},\bar{p},\bar{q},\bar{r} = 1,2,3,\ldots
\end{aligned} \tag{16}$$

Table 1
The characteristic boundary functions (CBF)

CBF	Fixed	Free	S-S[a]
$F_u(\xi,\eta)$	$F(\xi,\eta)$	1	1
$F_v(\xi,\eta)$	$F(\xi,\eta)$	1	1
$F_w(\xi,\eta)$	$F(\xi,\eta)$	1	$F(\xi,\eta)$

[a] Note: S-S means soft simply-supported boundary conditions.

Table 2
The Chebyshev polynomials for different mode categories

Geometric symmetry	Symmetric modes			Antisymmetric modes		
	U	V	W	U	V	W
x direction	$i=2,4,6,\ldots$	$l=1,3,5,\ldots$	$p=1,3,5,\ldots$	$i=1,3,5,\ldots$	$l=2,4,6,\ldots$	$p=2,4,6,\ldots$
y direction	$j=1,3,5,\ldots$	$m=2,4,6,\ldots$	$q=1,3,5,\ldots$	$j=2,4,6,\ldots$	$m=1,3,5,\ldots$	$q=2,4,6,\ldots$
z direction	$k=1,3,5,\ldots$	$n=1,3,5,\ldots$	$r=2,4,6,\ldots$	$k=2,4,6,\ldots$	$n=2,4,6,\ldots$	$r=1,3,5,\ldots$

in which

$$
\begin{aligned}
&D^{s,\bar{s},\tau,\bar{\tau}}_{\delta,\sigma,\theta,\bar{\delta},\bar{\sigma},\bar{\theta}} = \int_{-1}^{1}\int_{-1}^{1}\left\{\frac{\mathrm{d}^{s}}{\mathrm{d}\xi^{s}}\left[\frac{\mathrm{d}^{\tau}}{\mathrm{d}\eta^{\tau}}f_{\delta\sigma\theta}(\xi,\eta)\right]\frac{\mathrm{d}^{\bar{s}}}{\mathrm{d}\xi^{\bar{s}}}\left[\frac{d^{\bar{\tau}}}{\mathrm{d}\eta^{\bar{\tau}}}f_{\bar{\delta}\bar{\sigma}\bar{\theta}}(\xi,\eta)\right]\right\}\mathrm{d}\xi\,\mathrm{d}\eta,\\
&H^{s,\bar{s}}_{\delta_\varsigma\bar{\delta}_{\bar{\varsigma}}} = \int_{-1}^{1}\left\{\frac{\mathrm{d}^{s}P_{\varsigma}(\zeta)}{\mathrm{d}\zeta^{s}}\frac{\mathrm{d}^{\bar{s}}P_{\bar{\varsigma}}(\zeta)}{\mathrm{d}\zeta^{\bar{s}}}\right\}\mathrm{d}\zeta,\\
&f_{\delta\sigma\theta}(\xi,\eta) = F_{\delta}(\xi,\eta)P_{\sigma}(\xi)P_{\theta}(\eta),\\
&s,\bar{s},\tau,\bar{\tau}=0,1,\quad \delta,\bar{\delta}=u,v,w,\quad \sigma,\bar{\sigma}=i,l,p,\bar{i},\bar{l},\bar{p},\\
&\theta,\bar{\theta}=j,m,q,\bar{j},\bar{m},\bar{q},\quad \varsigma,\bar{\varsigma}=k,n,r,\bar{k},\bar{n},\bar{r}
\end{aligned}
\tag{17}
$$

For the common boundary conditions, the characteristic boundary functions $F_u(\xi,\eta)$, $F_v(\xi,\eta)$ and $F_w(\xi,\eta)$ are given in Table 1.

Considering the symmetry of the plates, eight distinct categories of vibration modes can be classified and each mode can be individually solved. This will greatly reduce the computational cost while maintaining the same level of accuracy. Using "A" to denote antisymmetric modes and "S" for symmetric modes, the eight categories can be written as AAA, AAS, ASA, ASS, SAA, SAS, SSA and SSS, where the three consecutive letters stand for the vibration categories in the x, y and z directions, respectively. The Chebyshev polynomial series in different directions are given in Table 2.

A non-trivial solution is obtained by setting the determinant of the coefficient matrix of Eq. (14) to zero. The roots of the determinant are the squares of the eigenvalues or non-dimensional eigenfrequencies. Eigenfunctions, i.e. mode shapes, are determined by back-substitution of the eigenvalues, one-by-one, in the usual manner. All computations are performed in double precision (16 significant figures) on a microcomputer. The integrals in Eq. (17) are numerically evaluated by the piecewise Gaussian quadrature with 24 points.

3. Convergence and comparison studies

In the Ritz method, it is very important to check its convergence and numerical robustness. The upper bound estimates of frequencies could be theoretically improved by continuously increasing the number of terms of admissible functions. However, a limit to the number of terms used in the computation always

Table 3
Convergence of the first eight frequency parameters of a fixed generalized super elliptical plate with powers $n_x = 1$, $n_y = 2$ and thickness ratio $h/b = 0.01$

$I \times J \times K$	Ω_1	Ω_2	Ω_3	Ω_4	Ω_5	Ω_6	Ω_7	Ω_8
AAA mode								
6×6×2	0.3651	0.7651	0.8727	1.249	1.500	1.618	1.853	2.207
7×7×2	0.3648	0.7645	0.8720	1.247	1.493	1.600	1.845	2.169
8×8×2	0.3647	0.7640	0.8716	1.247	1.492	1.598	1.844	2.162
8×8×3	0.3647	0.7640	0.8716	1.247	1.492	1.598	1.844	2.162
AAS mode								
6×6×1	4.549	5.921	8.256	8.360	9.532	11.66	11.93	12.25
7×7×1	4.549	5.920	8.256	8.360	9.529	11.66	11.92	12.24
8×8×1	4.549	5.918	8.256	8.360	9.527	11.66	11.92	12.24
8×8×2	4.549	5.918	8.256	8.360	9.527	11.66	11.92	12.24
ASA mode								
6×6×2	0.2335	0.5615	0.6631	0.9875	1.202	1.325	1.543	1.814
7×7×2	0.2333	0.5612	0.6626	0.9861	1.193	1.320	1.536	1.796
8×8×2	0.2332	0.5608	0.6622	0.9856	1.193	1.319	1.535	1.792
8×8×3	0.2332	0.5608	0.6622	0.9856	1.193	1.319	1.535	1.792
ASS mode								
6×6×1	3.893	6.389	7.942	9.735	10.29	10.54	11.19	13.01
7×7×1	3.892	6.389	7.939	9.733	10.29	10.54	11.19	13.01
8×8×1	3.891	6.388	7.938	9.733	10.29	10.54	11.18	13.01
8×8×2	3.891	6.388	7.938	9.733	10.29	10.54	11.18	13.01
SAA mode								
6×6×2	0.2369	0.5468	0.6810	0.9955	1.153	1.378	1.537	1.862
7×7×2	0.2368	0.5463	0.6803	0.9943	1.151	1.359	1.532	1.830
8×8×2	0.2366	0.5460	0.6799	0.9937	1.150	1.357	1.531	1.826
8×8×3	0.2366	0.5460	0.6799	0.9937	1.150	1.357	1.531	1.826
SAS mode								
6×6×1	3.925	6.342	7.859	9.758	10.21	10.72	11.13	13.20
7×7×1	3.924	6.342	7.857	9.757	10.21	10.72	11.13	13.19
8×8×1	3.923	6.342	7.855	9.756	10.21	10.72	11.12	13.19
8×8×2	3.923	6.342	7.855	9.756	10.21	10.72	11.12	13.19
SSA mode								
6×6×2	0.1139	0.4044	0.4361	0.7534	0.9616	1.000	1.254	1.473
7×7×2	0.1138	0.4040	0.4358	0.7527	0.9591	0.9920	1.250	1.462
8×8×2	0.1137	0.4037	0.4355	0.7523	0.9585	0.9914	1.249	1.460
8×8×3	0.1137	0.4037	0.4355	0.7523	0.9585	0.9914	1.249	1.460
SSS mode								
6×6×1	6.245	7.603	8.020	9.569	11.36	11.90	12.47	13.74
7×7×1	6.242	7.600	8.019	9.566	11.36	11.90	12.46	13.74
8×8×1	6.241	7.598	8.019	9.564	11.36	11.89	12.46	13.73
8×8×2	6.240	7.598	8.019	9.563	11.36	11.89	12.45	13.73

Table 4
Convergence of the first eight frequency parameters of a fixed generalized super elliptical plate with powers $n_x = 1$, $n_y = 2$ and thickness ratio $h/b = 0.2$

$I \times J \times K$	Ω_1	Ω_2	Ω_3	Ω_4	Ω_5	Ω_6	Ω_7	Ω_8
AAA mode								
5×5×3	4.181	6.999	7.664	9.713	10.75	10.90	11.26	11.75
6×6×3	4.181	6.998	7.661	9.704	10.74	10.84	11.17	11.69
7×7×3	4.180	6.997	7.660	9.703	10.74	10.84	11.17	11.68
7×7×4	4.179	6.995	7.658	9.700	10.74	10.84	11.16	11.68
AAS mode								
5×5×2	4.549	5.942	8.253	8.351	9.534	11.54	11.77	12.21
6×6×2	4.549	5.941	8.252	8.350	9.533	11.53	11.75	12.17
7×7×2	4.549	5.941	8.252	8.350	9.532	11.53	11.75	12.17
7×7×3	4.549	5.938	8.252	8.349	9.528	11.53	11.74	12.17
ASA mode								
5×5×3	2.987	5.655	6.336	8.329	9.445	9.985	10.63	11.13
6×6×3	2.986	5.654	6.335	8.323	9.388	9.942	10.62	11.08
7×7×3	2.986	5.654	6.334	8.323	9.383	9.940	10.62	11.08
7×7×4	2.985	5.652	6.332	8.321	9.381	9.938	10.62	11.08
ASS mode								
5×5×2	3.913	6.387	7.952	9.675	10.20	10.41	11.13	12.96
6×6×2	3.913	6.387	7.951	9.673	10.18	10.38	11.12	12.91
7×7×2	3.913	6.387	7.951	9.673	10.18	10.38	11.12	12.90
7×7×3	3.911	6.387	7.948	9.671	10.18	10.38	11.11	12.90
SAA mode								
5×5×3	3.021	5.567	6.446	8.359	9.205	10.23	10.70	11.10
6×6×3	3.020	5.567	6.442	8.355	9.192	10.11	10.66	11.07
7×7×3	3.020	5.566	6.442	8.355	9.191	10.10	10.66	11.07
7×7×4	3.019	5.565	6.440	8.353	9.189	10.10	10.66	11.06
SAS mode								
5×5×2	3.946	6.340	7.870	9.710	10.18	10.45	11.09	13.12
6×6×2	3.945	6.340	7.869	9.707	10.17	10.45	11.08	13.05
7×7×2	3.945	6.340	7.869	9.706	10.17	10.45	11.08	13.04
7×7×3	3.944	6.340	7.865	9.705	10.17	10.44	11.07	13.03
SSA mode								
5×5×3	1.712	4.445	4.746	6.946	8.118	8.352	9.734	10.79
6×6×3	1.711	4.444	4.744	6.944	8.103	8.299	9.714	10.72
7×7×3	1.711	4.444	4.744	6.944	8.103	8.296	9.713	10.71
7×7×4	1.711	4.443	4.743	6.942	8.100	8.293	9.710	10.71
SSS mode								
5×5×2	6.263	7.539	8.004	9.565	11.33	11.76	12.40	12.85
6×6×2	6.263	7.538	8.003	9.563	11.32	11.73	12.39	12.83
7×7×2	6.262	7.538	8.003	9.562	11.32	11.72	12.39	12.82
7×7×3	6.259	7.534	8.002	9.558	11.31	11.72	12.38	12.81

exists because of the limited numerical accuracy of computers, which greatly depends on the choice of global admissible functions. In the 3-D analysis, especially when the triplicate series has to be used, numerical instability may occur before the required accuracy of results is reached.

A generalized super elliptical plate with powers $n_x = 1$ and $n_y = 2$ enclosed within a square planform ($a/b = 1$) is taken as an example to show the convergence of the present method. The plate has a fixed

perimeter and two different thickness ratios ($h/b = 0.01$ and $h/b = 0.2$) are considered. It is obvious that $h/b = 0.01$ corresponds to a thin plate while $h/b = 0.2$ corresponds to a moderately thick plate. Tables 3 and 4 demonstrate the convergence of the first eight frequency parameters of each mode category for the two thickness ratios, respectively. For the plate with thickness ratio $h/b = 0.01$, 6–8 terms in the x and y directions are examined. However, only 2–3 terms in the z direction for the antisymmetric vibration and 1–2 terms for the symmetric vibration are examined. For the plate with thickness ratio $h/b = 0.2$, 5–7 terms in the x and y directions are examined. However, only 3–4 terms in the z direction for the antisymmetric vibration and 2–3 terms for the symmetric vibration are examined. It is seen that with increasing terms of Chebyshev polynomials used, the frequency parameters monotonically decrease and excellent convergence

Table 5
Comparison of the first two frequency parameters $\Omega = \omega a\sqrt{\rho/E}$ of fixed super elliptical plates with different powers and thickness ratios

h/b	$n_x = n_y$	Mode sequence number					
		AA-1	AA-2	AS(SA)-1	AS(SA)-2	SS-1	SS-2
0.01	1	0.4216	0.8400	0.2574	0.6163	0.1238	0.4220
		(0.4207)	(0.8378)	(0.2568)	(0.6148)	(0.1235)	(0.4208)
	2	0.3407	0.7392	0.2261	0.5214	0.1102	0.3990
		(0.3401)	(0.7379)	(0.2258)	(0.5202)	(0.1100)	(0.3981)
	4	0.3282	0.7304	0.2223	0.5007	0.1091	0.3977
		(0.3277)	(0.7289)	(0.2219)	(0.4996)	(0.1088)	(0.3969)
	10	0.3271	0.7298	0.2202	0.4982	0.1090	0.3976
		(0.3265)	(0.7285)	(0.2216)	(0.4973)	(0.1088)	(0.3968)
	∞	0.3271	0.7300	0.2221	0.4982	0.1090	0.3978
		(0.3265)	(0.7284)	(0.2216)	(0.4972)	(0.1088)	(0.3968)
		[0.3271]	[0.7300]	[0.2221]	[0.4982]	[0.1090]	[0.3977]
0.1	1	3.311	4.753*	2.173	4.119*	1.128	3.312
		(3.294)	(4.753)	(2.162)	(4.103)	(1.122)	(3.295)
	2	2.773	4.473*	1.934	3.821*	1.007	3.146
		(2.759)	(4.473)	(1.925)	(3.808)	(1.001)	(3.132)
	4	2.671	4.443*	1.898	3.754*	0.9927	3.134
		(2.659)	(4.442)	(1.889)	(3.742)	(0.9876)	(3.120)
	10	2.657	4.441*	1.894	3.740*	0.9911	3.133
		(2.644)	(4.440)	(1.884)	(3.728)	(0.9861)	(3.118)
	∞	2.657	4.441*	1.894	3.739*	0.9913	3.134
		(2.645)	(4.440)	(1.885)	(3.727)	(0.9864)	(3.120)
		[2.659]	[4.441]	[1.895]	[3.740]	[0.9920]	[3.135]
0.2	1	4.599	4.753*	3.212	4.129*	1.839	4.599
		(4.616)	(4.753)	(3.212)	(4.103)	(1.830)	(4.616)
	2	3.982	4.474*	2.910	3.830*	1.658	4.392
		(3.986)	(4.473)	(2.909)	(3.808)	(1.651)	(4.412)
	4	3.854	4.444*	2.857	3.748*	1.631	4.374
		(3.859)	(4.442)	(2.858)	(3.742)	(1.625)	(4.470)
	10	3.834	4.442*	2.850	3.748*	1.628	4.434
		(3.839)	(4.440)	(2.850)	(3.728)	(1.622)	(4.393)
	∞	3.833	4.442*	2.850	3.747*	1.628	4.374
		(3.840)	(4.440)	(2.851)	(3.727)	(1.622)	(4.395)
		[3.834]	[4.442]	[2.851]	[3.747]	[1.628]	[4.375]

Notes: Results in parentheses are from Liew et al. (1998b) using the higher-order shear deformation plate theory. Results in square brackets are from Liew et al. (1993) using the exact 3-D elasticity theory. The asterisk denotes symmetric modes in the thickness direction.

Table 6
Comparison of the first two frequency parameters $\Omega = \omega a\sqrt{\rho/E}$ of free super elliptical plates with different powers and thickness ratios

h/b	$n_x = n_y$	Mode sequence number					
		AA-1	AA-2	AS(SA)-1	AS(SA)-2	SS-1	SS-2
0.01	1	0.06479	0.2635	0.1502	0.2474	0.06478	0.1089
		(0.06477)	(0.2634)	(0.1502)	(0.2473)	(0.06476)	(0.1089)
	2	0.04877	0.2209	0.1226	0.2060	0.06029	0.08758
		(0.04876)	(0.2209)	(0.1226)	(0.2060)	(0.06027)	(0.08758)
	4	0.04324	0.2107	0.1112	0.1916	0.05940	0.07829
		(0.04322)	(0.2106)	(0.1112)	(0.1915)	(0.05940)	(0.07827)
	10	0.04115	0.2090	0.1063	0.1861	0.05928	0.07441
		(0.04113)	(0.2089)	(0.1063)	(0.1861)	(0.05928)	(0.07439)
	∞	0.04062	0.2088	0.1050	0.1846	0.05928	0.07341
		(0.04063)	(0.2089)	(0.1050)	(0.1847)	(0.05928)	(0.07341)
0.1	1	0.6196	2.286	1.372	2.186	0.6196	1.031
		(0.6193)	(2.281)	(1.370)	(2.178)	(0.6192)	(1.030)
	2	0.4641	1.940	1.129	1.857	0.5827	0.8378
		(0.4640)	(1.937)	(1.127)	(1.852)	(0.5823)	(0.8369)
	4	0.4101	1.855	1.024	1.739	0.5749	0.7521
		(0.4100)	(1.851)	(1.023)	(1.734)	(0.5746)	(0.7513)
	10	0.3899	1.840	0.9791	1.692	0.5737	0.7159
		(0.3898)	(1.837)	(0.9783)	(1.687)	(0.5734)	(0.7151)
	∞	0.3850	1.839	0.9670	1.679	0.5736	0.7064
		(0.3850)	(1.836)	(0.9663)	(1.675)	(0.5733)	(0.7059)
		[0.3851]	[1.839]	[0.9673]	[1.679]	[0.5736]	[0.7065]
0.2	1	1.126	2.909*	2.307	3.448	1.126	1.816
		(1.125)	(2.909)	(2.301)	(3.392)	(1.124)	(1.810)
		{1.126}	{2.909}	{2.307}	{3.448}	{1.126}	{1.816}
	2	0.8500	2.589*	1.932	3.008	1.072	1.504
		(0.8497)	(2.589)	(1.927)	(2.951)	(1.070)	(1.500)
	4	0.7534	2.481*	1.765	2.843	1.058	1.363
		(0.7531)	(2.481)	(1.762)	(2.716)	(1.057)	(1.359)
	10	0.7173	2.441*	1.693	2.775	1.056	1.302
		(0.7171)	(2.441)	(1.690)	(2.616)	(1.054)	(1.299)
	∞	0.7087	2.433*	1.673	2.589	1.055	1.286
		(0.7087)	(2.433)	(1.671)	(2.591)	(1.053)	(1.283)
		[0.7087]	[2.433]	[1.673]	[2.589]	[1.055]	[1.286]

Notes: Results in parentheses are from Liew et al. (1998b) using the higher-order shear deformation plate theory. Results in square brackets are from Liew et al. (1993) using the exact 3-D elasticity theory. Results in braces are from Zhou et al. (2003) using the exact 3-D elasticity theory. The asterisk denotes symmetric modes in the thickness direction.

has been achieved for all cases. It is shown that for a given accuracy, more terms of Chebyshev polynomials in the x and y directions than those in the z direction are needed, especially for thin plates. However, with increasing plate thickness, more terms of Chebyshev polynomials in the z direction should be used, with a decrease of terms needed in the x and y directions.

Results of the comparison studies are given in Tables 5 and 6 for super elliptical plates enclosed within square planforms with free and fixed boundaries, respectively. Three different thickness ratios ($h/b = 0.01$, 0.1, 0.3) and five groups of powers ($n_x = n_y = 1, 2, 4, 10, \infty$) have been examined. The solutions given by Liew et al. (1998b) from the higher-order shear deformation theory and the 3-D solutions for square plates given by Liew et al. (1993) and the 3-D solutions for circular plates given by Zhou et al. (2003) are used for comparison. It is seen that very good agreement has been observed for all cases and the maximum error between the present 3-D solutions and the 2-D higher-order theory is lower than 1%. From the tables, one

can find that in most cases, the present 3-D solutions are higher than the solutions of the 2-D higher-order plate theory.

4. Parametric study

In this section, the effects of geometric parameters such as the thickness ratio and the aspect ratio on the frequency parameters of plates are investigated. In Tables 7–9, the first six frequency parameters of each mode category are given for free generalized super elliptical plates with powers $n_x = 1$ and $n_y = 2$. Three different aspect ratios ($a/b = 0.5$, 1.0, 2.0) and four different thickness ratios ($h/b = 0.01$, 0.1, 0.2, 0.3) have been considered. It is seen that in all cases, the lowest frequency parameters are always provided by the SSA mode. In Figs. 2–5, the first four antisymmetric modes and the first three symmetric modes in the thickness direction for different mode categories of fixed generalized super elliptical

Table 7
The first six frequency parameters $\Omega = \omega a\sqrt{\rho/E}$ of each mode categories for free generalized super elliptical plates with powers $n_x = 1$, $n_y = 2$ and aspect ratio $a/b = 0.5$

h/b	Modes	Ω_1	Ω_2	Ω_3	Ω_4	Ω_5	Ω_6
0.01	AAA	0.05298	0.1970	0.4181	0.4866	0.6994	0.7775
	AAS	1.955	2.709	3.845	4.717	5.639	5.910
	ASA	0.1158	0.2989	0.4006	0.5513	0.6116	0.8673
	ASS	1.232	2.858	3.765	4.792	5.555	5.956
	SAA	0.09900	0.2126	0.2966	0.4287	0.5732	0.7536
	SAS	2.852	3.570	4.002	4.467	5.170	5.692
	SSA	0.03800	0.1508	0.1882	0.3075	0.4256	0.5776
	SSS	1.443	1.633	1.835	2.735	2.978	3.297
0.1	AAA	0.4808	1.622	3.017	3.395	4.452	4.781
	AAS	1.954	2.708	3.842	4.713	5.632	5.904
	ASA	1.011	2.304	2.945	3.733	4.041	5.196
	ASS	1.232	2.858	3.762	4.786	5.548	5.936
	SAA	0.8894	1.742	2.296	3.085	3.839	4.719
	SAS	2.852	3.561	3.994	4.455	5.152	5.686
	SSA	0.3643	1.310	1.572	2.362	3.059	3.880
	SSS	1.706	3.222	3.526	4.171	4.884	5.628
0.2	AAA	0.8084	2.401	3.999	4.139	4.991	5.249
	AAS	1.954	2.704	3.831	4.700	5.584	5.838
	ASA	1.601	3.217	3.716	4.601	4.875	5.153
	ASS	1.231	2.854	3.754	4.758	5.520	5.794
	SAA	1.445	2.560	3.200	4.002	4.838	5.080
	SAS	2.851	3.530	3.962	4.407	5.060	5.658
	SSA	0.6595	2.041	2.349	3.262	4.084	4.809
	SSS	1.704	3.194	3.512	4.126	4.856	5.411
0.3	AAA	0.9925	2.754	3.369	3.711	4.365	4.409
	AAS	1.952	2.697	3.785	4.606	4.780	4.854
	ASA	1.903	3.261	3.574	3.584	4.289	5.003
	ASS	1.230	2.847	3.730	4.473	4.785	5.005
	SAA	1.742	2.875	3.351	3.708	4.293	4.761
	SAS	2.850	3.442	3.856	4.284	4.554	4.913
	SSA	0.8959	2.416	2.697	3.473	4.103	4.512
	SSS	1.702	3.126	3.478	3.968	4.554	4.785

Table 8
The first six frequency parameters $\Omega = \omega a\sqrt{\rho/E}$ of each mode categories for free generalized super elliptical plates with powers $n_x = 1$, $n_y = 2$ and aspect ratio $a/b = 1.0$

h/b	Modes	Ω_1	Ω_2	Ω_3	Ω_4	Ω_5	Ω_6
0.01	AAA	0.05426	0.2347	0.3516	0.5178	0.7570	0.8657
	AAS	2.7010	5.412	5.547	5.982	7.867	8.490
	ASA	0.1354	0.2161	0.3655	0.5587	0.6416	0.7102
	ASS	3.177	4.258	6.415	6.734	7.181	8.133
	SAA	0.1306	0.2253	0.3633	0.5344	0.6731	0.7011
	SAS	3.102	4.210	6.572	6.866	7.263	7.980
	SSA	0.06174	0.09594	0.2363	0.3938	0.4234	0.5223
	SSS	2.821	4.043	4.383	5.565	7.812	8.619
0.1	AAA	0.5175	2.054	2.969	4.080	5.600	6.261
	AAS	2.701	5.410	5.544	5.982	7.861	8.478
	ASA	1.246	1.937	3.040	4.390	4.936	5.292
	ASS	3.176	4.257	6.409	6.728	7.160	8.128
	SAA	1.197	2.012	3.021	4.228	5.140	5.227
	SAS	3.102	4.210	6.566	6.861	7.240	7.974
	SSA	0.5951	0.9140	2.072	3.283	3.508	4.110
	SSS	2.821	4.037	4.381	5.563	7.806	8.607
0.2	AAA	0.9455	3.260	4.448	5.807	7.458	8.073
	AAS	2.701	5.401	5.536	5.982	9.838	8.427
	ASA	2.121	3.116	4.551	6.125	6.751	7.153
	ASS	3.173	4.256	6.385	6.703	7.087	8.111
	SAA	2.035	3.217	4.522	5.943	6.949	7.102
	SAS	3.099	4.209	6.545	6.841	7.154	7.954
	SSA	1.091	1.628	3.294	4.837	5.135	5.839
	SSS	2.821	4.016	4.372	5.559	7.787	8.554
0.3	AAA	1.272	3.897	5.022	6.406	6.642	7.472
	AAS	2.700	5.380	5.519	5.980	7.762	8.200
	ASA	2.672	3.707	5.263	6.518	6.615	7.182
	ASS	3.169	4.255	6.323	6.619	6.932	8.058
	SAA	2.565	3.804	5.213	6.395	6.668	7.201
	SAS	3.095	4.207	6.484	6.789	6.950	7.902
	SSA	2.103	3.958	5.375	5.740	6.503	7.675
	SSS	2.821	3.978	4.354	5.551	7.728	8.294

plates with aspect ratio $a/b = 1$ and powers $n_x = 1$ and $n_y = 3$ have been plotted with respect to the thickness ratio h/b. It is shown that the effect of thickness ratio on the frequency parameters of antisymmetric modes in the thickness direction is much larger than those of symmetric modes. In the range of h/b from 0.01 to 0.3, the first three frequency parameters of the SSA modes and the first ones of the ASA, SAA and AAA modes all monotonically increase with the thickness ratio. The first two frequency parameters of the AAS, ASS and SAS modes and the first one of the SSS modes are basically insensitive to the thickness ratio. In general, the frequency parameters of the antisymmetric modes in the thickness direction increase with the plate thickness. However, the frequency parameters of the symmetric modes in the thickness direction decrease when the plate thickness increases. Therefore, one can conclude that for thin plates the frequencies of symmetric modes in the thickness direction are much higher than those of antisymmetric modes and are all within the higher range of frequencies. However, with the increase in plate thickness, the frequencies of symmetric modes in the thickness direction gradually decrease and fall into the lower range of frequencies.

Table 9
The first six frequency parameters $\Omega = \omega a\sqrt{\rho/E}$ of each mode categories for free generalized super elliptical plates with powers $n_x = 1$, $n_y = 2$ and aspect ratio $a/b = 2.0$

h/b	Modes	Ω_1	Ω_2	Ω_3	Ω_4	Ω_5	Ω_6
0.01	AAA	0.05335	0.1902	0.4092	0.5086	0.7036	0.7706
	AAS	3.877	5.266	7.534	9.272	11.36	11.89
	ASA	0.09584	0.2222	0.2940	0.4170	0.5787	0.7211
	ASS	5.733	7.196	7.970	8.892	10.13	11.38
	SAA	0.1127	0.2889	0.4122	0.5495	0.6254	0.8673
	SAS	2.378	5.595	7.380	9.545	10.97	12.28
	SSA	0.03642	0.1575	0.1831	0.3076	0.4267	0.5540
	SSS	3.361	6.546	7.181	8.409	9.743	10.87
0.1	AAA	0.5140	1.778	3.637	4.460	5.902	6.389
	AAS	3.877	5.265	7.533	9.270	11.36	11.89
	ASA	0.9303	2.079	2.705	3.717	4.984	6.069
	ASS	5.733	7.192	7.966	8.887	10.12	11.37
	SAA	1.073	2.637	3.709	4.745	5.340	7.067
	SAS	2.378	5.594	7.379	9.543	10.97	12.26
	SSA	0.3599	1.507	1.734	2.810	3.802	4.807
	SSS	3.360	6.542	7.179	8.404	9.739	10.85
0.2	AAA	0.9636	3.115	5.874	7.001	8.870	9.439
	AAS	3.876	5.264	7.529	9.266	11.35	11.87
	ASA	1.730	3.617	4.561	6.002	7.705	9.103
	ASS	5.733	7.177	7.957	8.872	10.09	11.36
	SAA	1.952	4.435	6.001	7.378	8.133	10.32
	SAS	2.378	5.593	7.376	9.535	10.96	12.22
	SSA	0.6987	2.719	3.074	4.714	6.230	7.875
	SSS	3.360	6.531	7.172	8.386	9.729	10.80
0.3	AAA	1.331	4.019	7.119	8.182	10.20	10.63
	AAS	3.875	5.262	7.521	9.257	11.33	11.84
	ASA	2.358	4.633	5.687	7.245	9.056	10.41
	ASS	5.732	7.149	7.938	8.844	10.03	11.34
	SAA	2.610	5.536	7.170	8.712	9.309	11.54
	SAS	2.377	5.590	7.371	9.518	10.95	12.11
	SSA	1.003	3.596	3.992	5.852	7.389	8.793
	SSS	3.358	6.509	7.160	8.352	9.702	10.69

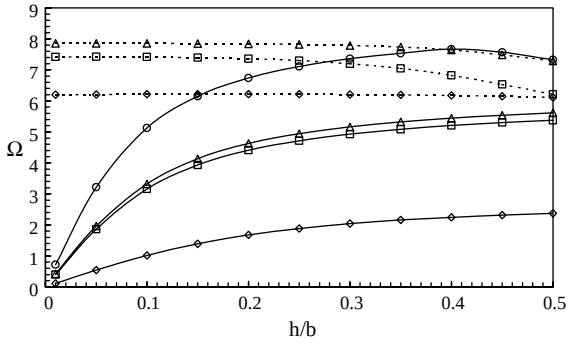

Fig. 2. The first four SSA modes and the first three SSS modes of fixed generalized super elliptical plates with aspect ratio $a/b = 1$ and powers $n_x = 1$ and $n_y = 3$ ((—◇—) SSA-1, (—□—) SSA-2, (—△—) SSA-3, (—○—) SSA-4, (···◇···) SSS-1, (···□···) SSS-2 and (···△···) SSS-3).

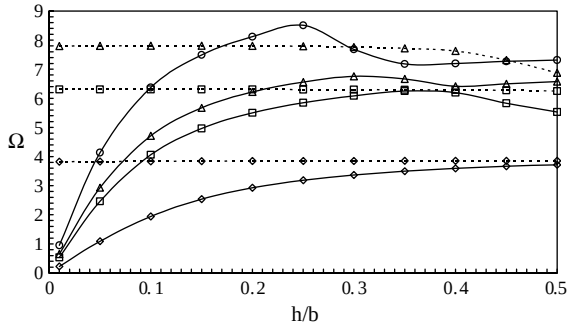

Fig. 3. The first four ASA modes and the first three ASS modes of fixed generalized super elliptical plates with aspect ratio $a/b = 1$ and powers $n_x = 1$ and $n_y = 3$ ((◇) ASA-1, (□) ASA-2, (△) ASA-3, (○) ASA-4, (◇) ASS-1, (□) ASS-2 and (△) ASS-3).

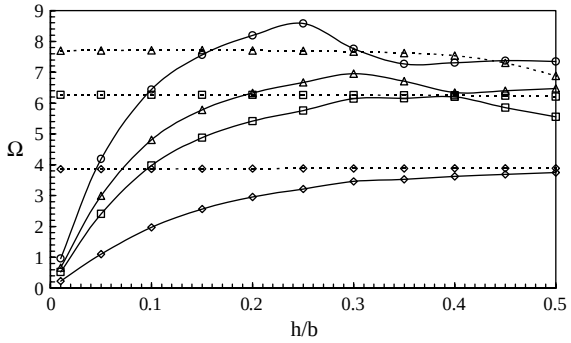

Fig. 4. The first four SAA modes and the first three SAS modes of fixed generalized super elliptical plates with aspect ratio $a/b = 1$ and powers $n_x = 1$ and $n_y = 3$ ((◇) SAA-1, (□) SAA-2, (△) SAA-3, (○) SAA-4, (◇) SAS-1, (□) SAS-2 and (△) SAS-3).

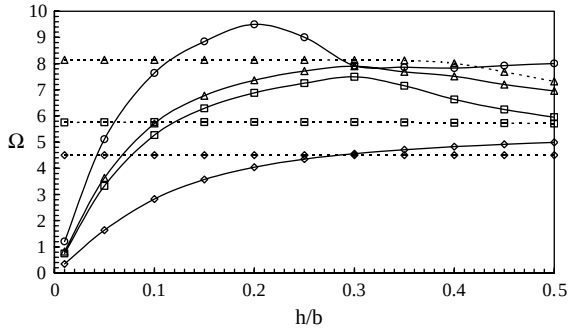

Fig. 5. The first four AAA modes and the first three AAS modes of fixed generalized super elliptical plates with aspect ratio $a/b = 1$ and powers $n_x = 1$ and $n_y = 3$ ((◇) AAA-1, (□) AAA-2, (△) AAA-3, (○) AAA-4, (◇) AAS-1, (□) AAS-2 and (△) AAS-3).

5. Concluding remarks

In this paper, the 3-D vibration of generalized supper elliptical plates has been investigated by the Chebyshev–Ritz method. The analysis is based on the exact, small strain and linear elasticity theory.

The product of a triplicate Chebyshev polynomial series and a characteristic boundary function is taken as the admissible function for each displacement component. The triplicate Chebyshev polynomial series is defined in a rectangular hexahedron enclosing the plate under consideration while the characteristic boundary function ensures the exact satisfaction of the geometric boundary conditions of the plate. Convergence and comparison studies demonstrate the accuracy and validity of the present method. The effect of various geometric parameters on frequency parameters has also been studied.

Acknowledgements

The work described in this paper was partially supported by a grant "Analysis of building structures using hybrid stress hexahedral elements" from the Research Grants Council of the Hong Kong Special Administrative Region, China (Project No: HKU7071/99E).

References

Chen, C.C., Lim, C.W., Kitipornchai, S., Liew, K.M., 1999. Vibration of symmetrically laminated thick super elliptical plates. Journal of Sound and Vibration 220, 659–682.

Chen, C.C., Kitipornchai, S., Lim, C.W., Liew, K.M., 2000. Free vibration of symmetrically laminated thick-perforated plates. Journal of Sound and Vibration 230, 111–132.

Cheung, Y.K., Zhou, D., 2002. Three-dimensional vibration analysis of cantilevered and completely free isosceles triangular plates. International Journal of Solids and Structures 39, 673–687.

DeCapua, N.J., Sun, B.C., 1972. Transverse vibration of a class of orthotropic plates. Journal of Applied Mechanics—ASME 39, 613–615.

Irie, T., Yamada, G., Sonoda, M., 1983. Natural frequencies of square membrane and square plate with rounded corners. Journal of Sound and Vibration 100, 83–89.

Leissa, A., Jacob, K.I., 1986. Three-dimensional vibrations of twisted cantilevered parallelepipeds. Journal of Applied Mechanics—ASME 53, 614–618.

Leissa, A.W., Zhang, Z.D., 1983. On the three-dimensional vibrations of the cantilevered rectangular parallelepiped. Journal of the Acoustical Society of America 73, 2013–2021.

Liew, K.M., Feng, Z.C., 2001. Three-dimensional free vibration analysis of perforated super elliptical plates via the p-Ritz method. International Journal of Mechanical Sciences 43, 2613–2630.

Liew, K.M., Yang, B., 2000. Elasticity solutions for free vibrations of annular plates from three-dimensional analysis. International Journal of Solids and Structures 37, 7689–7702.

Liew, K.M., Hung, K.C., Lim, M.K., 1993. A Continuum three-dimensional vibration analysis of thick rectangular plates. International Journal of Solids and Structures 30, 3357–3379.

Liew, K.M., Hung, K.C., Lim, M.K., 1994. Three-dimensional elasticity solutions to vibration of cantilevered skewed trapezoids. AIAA Journal 32, 2080–2089.

Liew, K.M., Hung, K.C., Lim, M.K., 1995a. Modeling three-dimensional vibration of elliptic bars. Journal of the Acoustical Society of America 98, 1518–1526.

Liew, K.M., Hung, K.C., Lim, M.K., 1995b. Vibration characteristics of simply supported thick skew plates in three-dimensional setting. Journal of Applied Mechanics—ASME 62, 880–886.

Liew, K.M., Hung, K.C., Lim, M.K., 1998a. Vibration of thick prismatic structures with three-dimensional flexibility. Journal of Applied Mechanics—ASME 65, 619–625.

Liew, K.M., Kitipornchai, S., Lim, C.W., 1998b. Free vibration analysis of thick super-elliptical plates. Journal of Engineering Mechanics—ASCE 124, 137–145.

Lim, C.W., Liew, K.M., 1995. Vibrations of perforated plates with rounded corners. Journal of Engineering Mechanics-ASCE 121, 203–213.

Lim, C.W., Kitipornchai, S., Liew, K.M., 1998. Free vibration analysis of doubly connected super elliptical laminated composite plates. Composite Science and Technology 58, 435–445.

Narita, Y., 1985. Natural frequencies of free, orthotropic elliptical plates. Journal of Sound and Vibration 100, 83–89.

Rajalingham, C., Bhat, R.B., Xistris, G.D., 1993. Natural frequencies and mode shapes of elliptic plates with boundary characteristic orthogonal polynomials as assumed shape functions. Journal of Vibration and Acoustics—ASME 115, 353–358.

Sato, K., 1971. Free flexural vibration of an elliptical plate with simply supported edge. Journal of the Acoustical Society of America 52, 919–922.

So, J., Leissa, A.W., 1998. Three-dimensional vibrations of thick circular and annular plates. Journal of Sound and Vibration 209, 15–41.

Wang, C.M., Wang, L., Liew, K.M., 1994. Vibration and buckling of super elliptical plates. Journal of Sound and Vibration 171, 301–314.

Young, P.G., Dickinson, S.M., 1994. Free vibration of a class of solids with cavities. International Journal of Mechanical Sciences 36, 1099–1107.

Young, P.G., Dickinson, S.M., 1995. Free vibration of a class of homogeneous isotropic solids. Journal of Applied Mechanics—ASME 62, 706–708.

Zhou, D., Cheung, Y.K., Au, F.T.K., Lo, S.H., 2002. Three-dimensional vibration analysis of thick rectangular plates using Chebyshev polynomial and Ritz method. International Journal of Solids and Structures 39, 6339–6353.

Zhou, D., Au, F.T.K., Cheung, Y.K., Lo, S.H., 2003. Three-dimensional vibration analysis of circular and annular plates via the Chebyshev–Ritz method. International Journal of Solids and Structures 40 (12), 3089–3105.